

Indentation experiments on silica optical fibers

Bochien Lin
M. John Matthewson
Gregory J. Nelson

Fiber Optic Materials Research Program, Rutgers University,
P.O. Box 909, Piscataway, N.J. 08855-0909

ABSTRACT

Kilometer lengths of optical fiber have a much lower strength than short lengths due to occasional defects of an extrinsic nature. The fatigue properties of these defects are hard to study due to their rarity. Subthreshold indentation flaws in silica optical fibers (*i.e.* Vickers indentations produced under sufficiently low load to avoid radial crack formation) have been shown to exhibit environmental fatigue similar to "pristine" silica fiber. Thus the indentation technique may be used to introduce controlled flaws into the fiber that model the strength limiting defects found in long length specimens. This paper presents the results of fatigue studies on subthreshold indentation flaws that have strengths of up to ~ 1 GPa (typical of proof stress levels).

1. INTRODUCTION

Optical fibers have achieved tremendous success in long distance telecommunication applications and fiber cables represent a major capital investment for the communications industry. Clearly, the reliability of the fibers is extremely important and especially so for sub-ocean cables which are far less accessible for repair than terrestrial cables. It is therefore necessary to understand the mechanical behavior of high quality optical fibers such as strength distribution, strength degradation factors and fatigue behavior. The longest convenient laboratory test length for fiber strength measurement is typically a few meters for a tensile test, while bending tests, which are far more convenient to use, have an effective test length of only a few tens of microns. Such tests give limited information about the strength of the kilometer lengths used in optical cables. From the weakest link model, the longer the fiber, the lower the strength will be. In fact, for the kilometer length fibers the flaws are usually "extrinsic" in nature and may originate from handling damage or particles which become adhered to the surface during the drawing process. In contrast, for short length fibers, the intrinsic strength seems close to "perfect".¹

Currently, the standard subcritical crack growth model is widely used to predict the lifetime by extrapolating from accelerated testing on short lengths to the lower applied stress and the lower initial strength typical of optical fiber in field use. The problems are i) no cracks exist in the "pristine fiber" ii) there are no empirical data relating time to failure and initial strength for weak fibers. It is therefore dangerous to extrapolate the fatigue data for pristine fibers to the weak fibers. For high strength fibers, the stress corrosion parameter, n , is around 20, while for bulk glass containing well defined cracks n is around 40. Also, at least in liquid water, fibers exhibit a lower value of n at low applied stress/long time to failure which shows as a "knee" in the static fatigue behavior. The reason for anomalous fiber behavior is not clear (see Ref. 2 for a discussion of likely mechanisms). There have been few studies published on the fatigue properties of weaker fiber. A review of the literature³ found little correlation between the fiber strength and the n value for fiber in the strength range 0.5 - 7 GPa. Recently, Yuce, Colucci, Key and Andrejco⁴ weakened fibers by incorporating hard particles in the polymer coating and found that the fibers had similar n values to "pristine" fibers, but in general it is difficult to control and determine the severity of this kind of flaw.

An indentation technique, which involves loading a Vickers diamond pyramid onto the glass, provides an interesting method for introducing controlled flaws and, in addition, indentation is known to be a good model for handling and abrasion damage. Also, residual stresses are associated with the indentations, so that the technique is a plausible model for the behavior of particles which adhere to the fiber surface during drawing and which produce a residual stress field on cooling due to a thermal expansion mismatch. Dabbs and Lawn⁵ found that indentation flaws could be classified into two types as shown in Fig. 1. The pointed indenter causes plastic deformation in the glass which leaves a residual stress field upon unloading. At high indentation loads, radial cracks form in silica on loading⁶ and these indentations are called

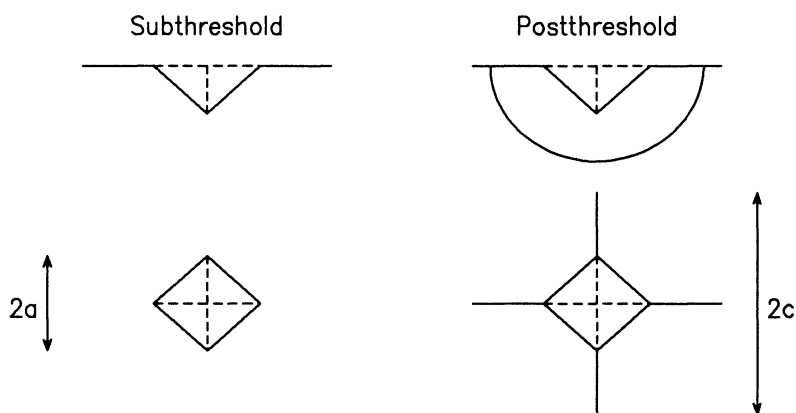


Fig. 1. Schematic diagram of the sub- and postthreshold indentation flaws shown in section (top) and plan (bottom).

"postthreshold" flaws (where the threshold is with respect to the radial crack formation). At lower loads no radial cracks form and these flaws are classified as "subthreshold". Dabbs and Lawn measured the dynamic fatigue parameter, n , for these flaws and found $n \sim 20$ for subthreshold flaws and $n \sim 30$ for postthreshold flaws, as shown in Fig. 2. They suggested that the residual stresses influence the dynamic fatigue response. They noted that, in the transition region, radial cracks could spontaneously "pop-in" giving a postthreshold flaw. They suggested this as a possible mechanism for the "knee" in the fatigue observed for high strength fiber. However, Matthewson and Kurkjian⁷ show that extrapolation of pop-in data gives times to pop-in that are too long and there would need to be an unreasonably large number of such flaws. However, the pop-in phenomena may be important since proof testing does not assure a given strength because subsequent pop-in of subthreshold flaws can cause spontaneous loss of strength. The initiation of cracks from defects such as shear lines generated in the highly inhomogeneous elastic/plastic contact field can theoretically explain the crack pop-in behavior.⁸ However, there still remains work to be done to understand how these indentations relate to fatigue behavior of high strength fiber. Also, from the previous work^{5,9} there are still some questions such as i) the published work uses glass rods tested in four point bending for the postthreshold indents while glass fiber tested in tension is used for the subthreshold indents. It is therefore not possible to uniquely assign the discontinuity in behavior at the threshold to only changes in the character of the flaws. ii) the strongest indented fibers have an inert strength of $\sim 4\%$ strain to failure while the strain to failure of pristine fiber is $\sim 20\%$ leaving a gap in the data in the region of most interest. iii) the previous work used dynamic fatigue and did not consider static fatigue over long periods of time.

The purpose of this study is to explore the whole range of indentation load from postthreshold down to loads giving strengths as close as possible to the "pristine" fiber and to investigate static fatigue behavior. In particular, it is important to determine whether weaker fibers exhibit a "knee" in the fatigue curve, which would have serious practical implications.

2. EXPERIMENTAL

For postthreshold indentations, the fibers tested need to be thick enough to withstand the high indent load without spontaneous failure, while for subthreshold flaws the fibers need to be flexible enough and hence thin enough not break while loading into the two point bend apparatus described below. For these reasons, six different diameter fibers, ranging from 100 to 1000 μm , have been used in these experiments. A preliminary experiment was conducted for unindented polymer coated fibers to see whether there are intrinsic differences between fibers of different diameters brought about by the different draw conditions which might perturb the indentation results. The fused silica fibers with core diameter 100, 200, 300, 400, 600 and 1000 μm coated with UV-curable polyurethane acrylate were tested in the two point bending

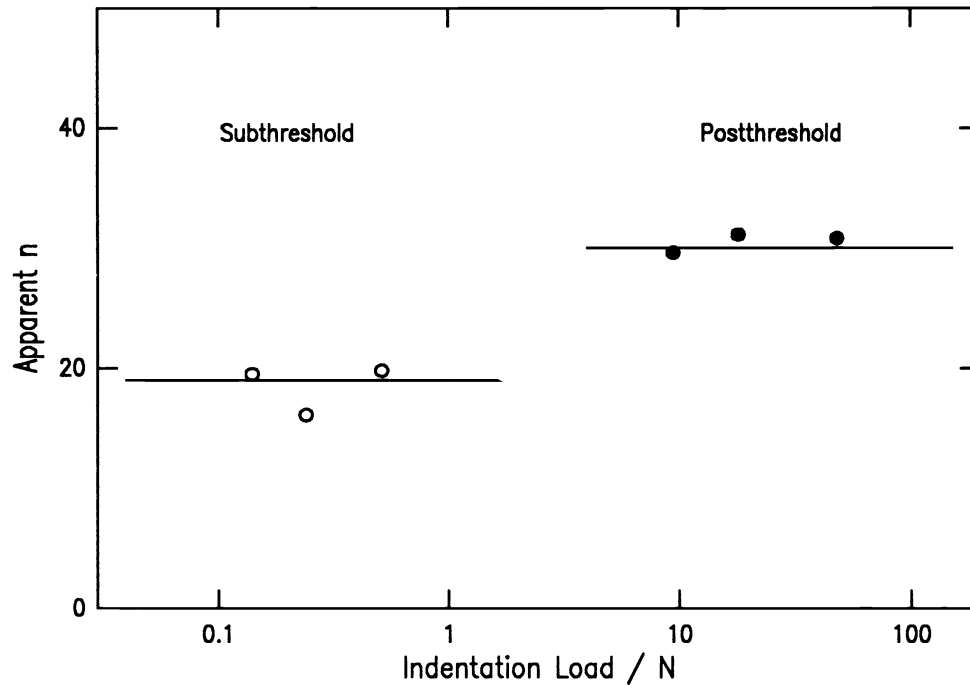


Fig. 2. Apparent stress corrosion parameter, n , versus indentation load in a semi-log scale (data from Ref. 5).

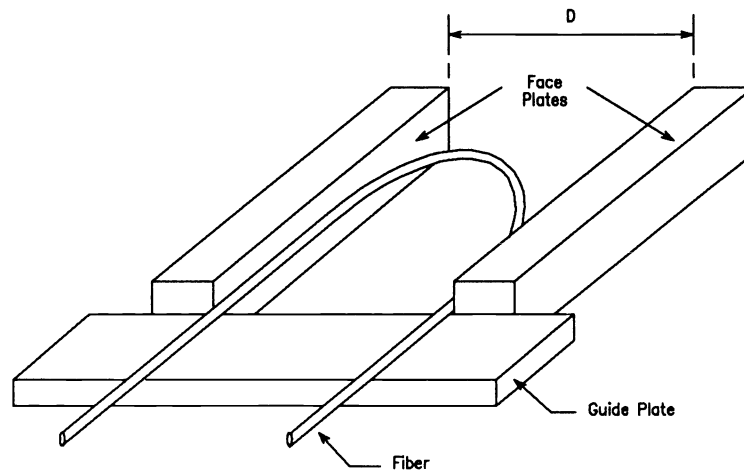


Fig. 3. Schematic of the two point bend apparatus for determining fiber strength.

apparatus, Fig. 3.¹⁰ This is the only technique available for studying such a wide range of fiber diameter. To provide a reproducible environment, the fibers were soaked in a pH 7 buffer solution for 24 hours before testing in order to allow equilibration of the pH and water availability at the silica surface. They were then tested while still wetted with pH 7 buffer solution. To get a fair comparison between the different diameters the dynamic fatigue test was run under constant strain rate rather than constant jaw speed.¹¹ The strain rates used were 0.05, 0.2, 1 and 5 %/min. Ten specimens for each diameter were tested for each strain rate. A plot of failure strain, ϵ_f , versus fiber diameter is shown in Fig. 4 for each strain rate. The strain to failure is calculated as from

$$\epsilon_f = 1.198 \frac{d}{D-d}, \quad (1)$$

where d is the fiber diameter, d' is the overall fiber diameter including the coating and D is the face plate separation at failure.¹² It is seen that, although there is some scatter, the strain to failure does perhaps show a trend downwards with increasing diameter. However the thicker fibers have a greater surface area under stress so that the weakest link model for strength would predict a lower strength. The total fiber surface area under test at a given strain is proportional to d^2 ; since both the fiber circumference and the test length are proportional to d for a given applied strain. To correct for this size effect Fig. 5 shows corrected strain, ϵ_{fc} , which is given by

$$\epsilon_{fc} = \epsilon_f \left(\frac{d}{d_{100}} \right)^{2/m}. \quad (2)$$

The correction factor is normalized to the 100 μm diameter fiber to retain non-dimensionality and assumes Weibull statistics for the weakest link model. The value of the Weibull modulus m is calculated separately for each point and was typically found to be in the range of 60 to 180. There is now no apparent diameter dependence of ϵ_{fc} so that the trend observed in Fig. 4 is simply due to different specimen sizes and there is no evidence of intrinsic strength differences. Any such effects are dominated by the random preform to preform variation. The stress corrosion parameter, n , calculated for each diameter is shown in Fig. 6 and again there is no systematic variation with diameter. We therefore conclude that basically these six different diameter fibers are essentially the same material even though the drawing conditions were somewhat different for each fiber.

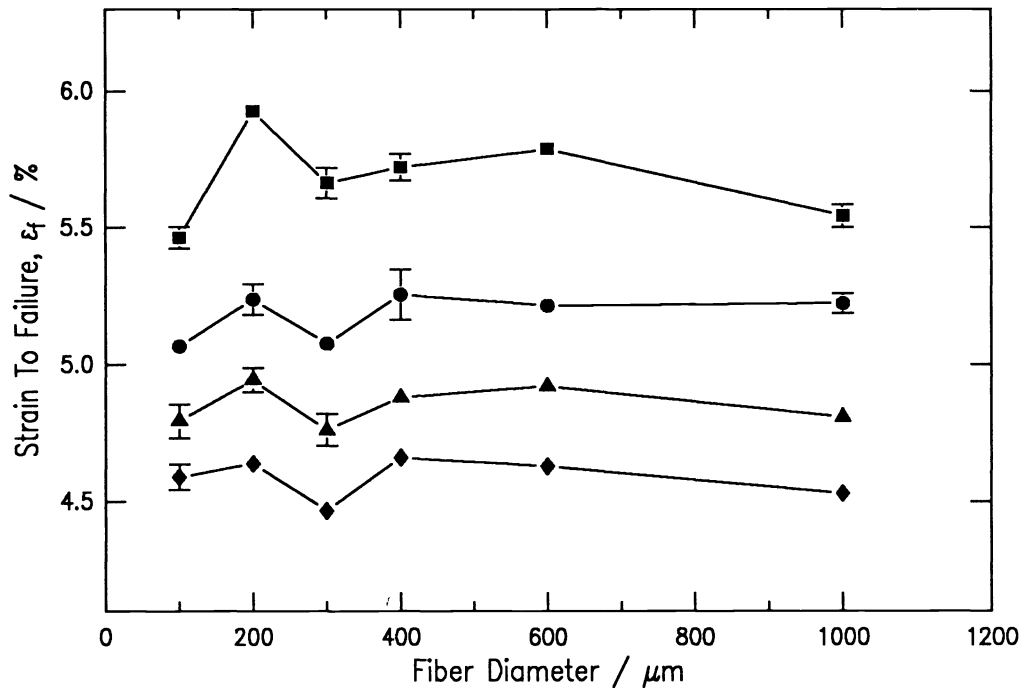


Fig. 4. Plot of strain to failure versus diameter of coated unindented fiber. Key: strain rates \blacksquare 5, \bullet 1, \blacktriangle 0.2 and \blacklozenge 0.05%/min.

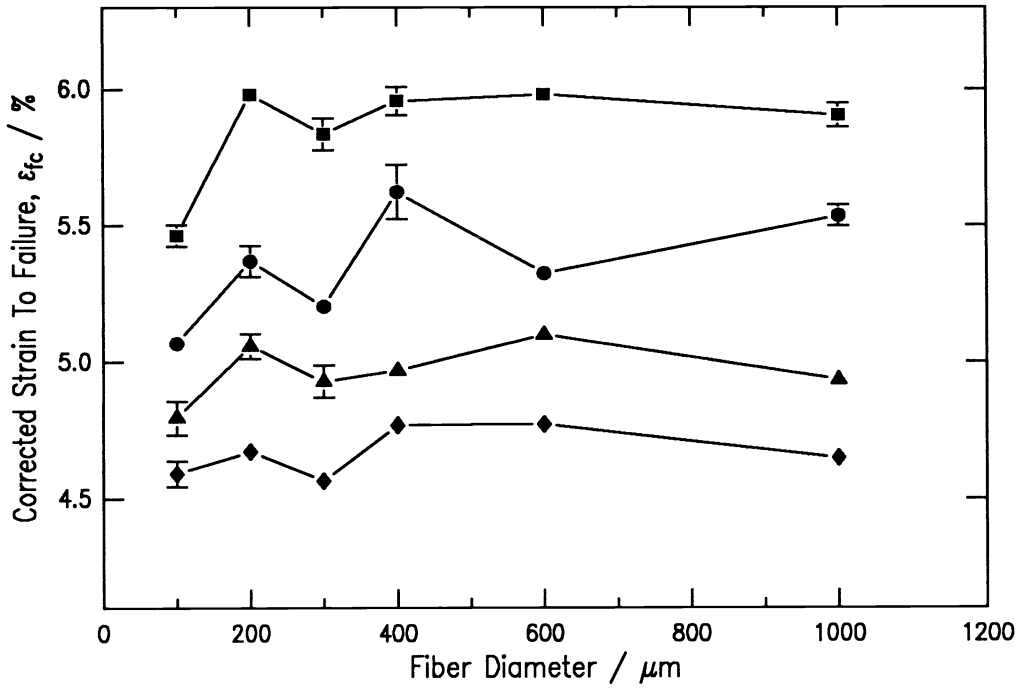


Fig. 5. Plot of corrected strain to failure, ϵ_{fc} , versus diameter of polymer coated unindented fiber. See Fig. 4 for key.

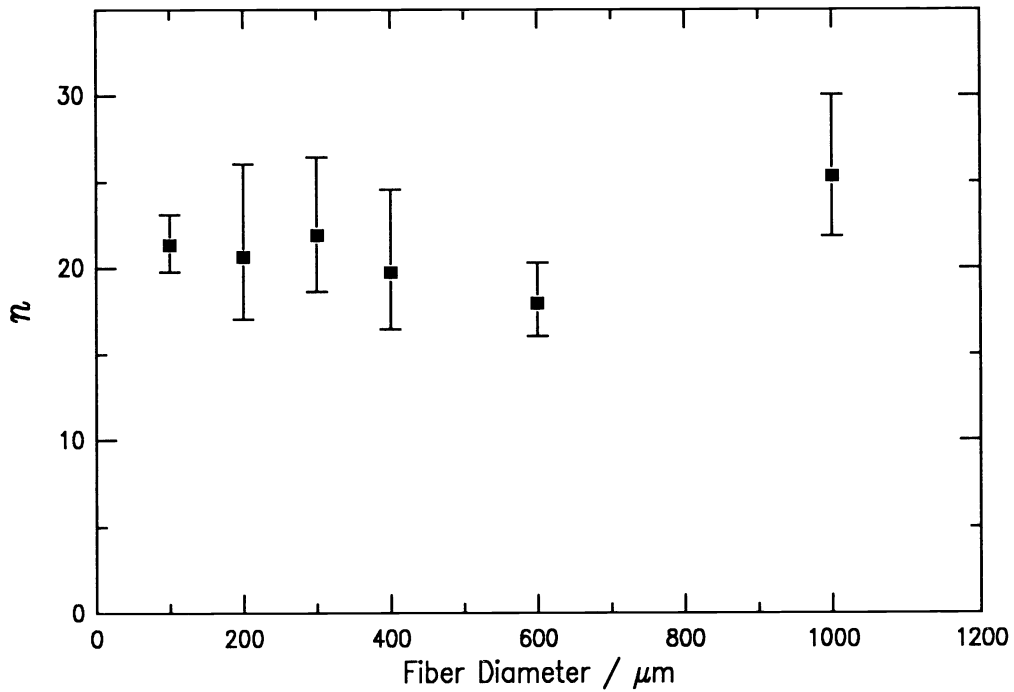


Fig. 6. Dynamic stress corrosion parameter, n , versus fiber diameter.

The polymer coating was stripped from each fiber prior to indentation with hot sulfuric acid followed by a rinse in acetone for a few seconds. A "flag" was attached to one end of the fiber to serve as an indicator of the indentation direction to ensure that the indent could be positioned in the maximum tensile region when measuring the strength by bending. The fiber was then mounted on a rigid substrate ready for indentation. A Leco M-400-G3 microindentation machine equipped with a Vickers diamond pyramid indenter was used to make indentations with loads ranging from 10 mN to 5 N (1 to 500 gf) and held under peak load for 10 seconds in air. After unloading the dimensions of the plastic indentation zone, a , and crack lengths, c , (if present) were measured where a and c are defined in Fig 1. The strength of the indented fiber was then measured using either the two-point bend apparatus for stronger/thinner fibers or a purpose built four point bend apparatus for weaker/thicker fibers. This latter apparatus, shown schematically in the Fig. 7, involves threading the fiber between four pins, the center two of which are then moved under computer control until the fiber breaks. This apparatus has recently been used successfully to measure the strength of fluoride fibers down to liquid nitrogen temperatures;¹³ an experiment that would have been very difficult to perform using any other technique. During indentation the rear surface of the fiber is pressed against the support block and can be severely damaged. Strength measurement in bending has been used throughout this work so that this damaged region is only subjected to compressive stresses and can not influence the results by causing premature failure. The fractured ends of the broken fibers were examined using a microscope to verify that failure had indeed initiated from the indentations. Ten specimens were tested for each load.

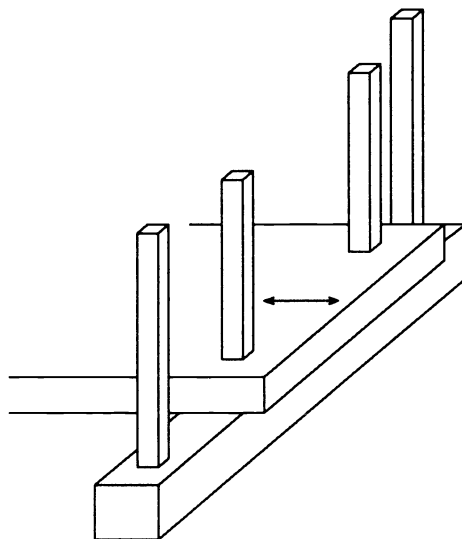


Fig. 7. Schematic diagram of the four point bend apparatus for determining fiber strength.

3. RESULTS AND DISCUSSION

Fig. 8 shows the dimensions of the plastic indentation zone, a , and crack lengths, c , from this work and are compared with results from Dabbs, Marshall and Lawn¹⁴ for a borosilicate fiber. The results for a are similar though there is a slight shift due the different hardness and Young's modulus of these two materials. However, the threshold load for radial crack formation is much higher for silica and is attributed to the fact that the two materials have a different structure and short range order. The threshold load for the silica is close the estimated value derived by Jakus *et al.*⁹ The advantage of our experiments is that we can extend down to lower loads of more practical interest. The hardness was found to be load independent in our study for all loads, *i.e.* the slope of a versus P is $\sim 1/2$ in Fig. 8.

Fig. 9 shows a double log plot of strain to failure, ϵ_f , in ambient environment versus indent load, P , at a strain rate of 0.036 %/min for dynamic fatigue testing in both two point bending (in the subthreshold range) and four point bending (in the transition and postthreshold regions). Also shown are Jakus' inert strengths for subthreshold flaws. Bimodal behavior was observed in the four point bend results for loads near the threshold region. The strength distributions at indentation loads less than 0.5 N were found to be unimodal, which implies a single initiation controlled mechanism of failure. But

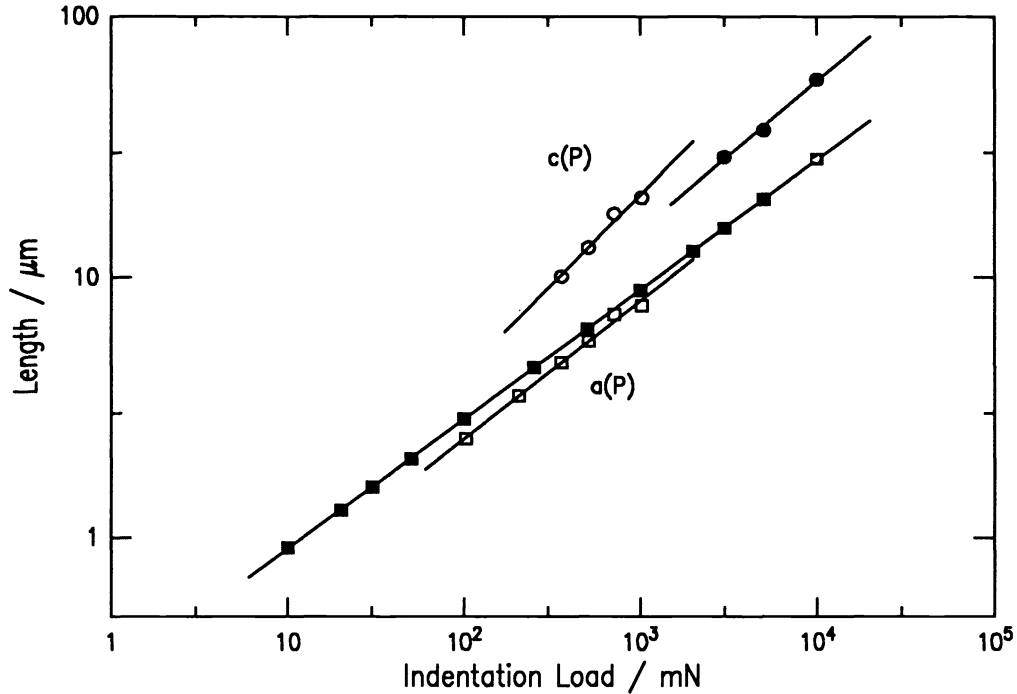


Fig. 8. Indentation size, a , and radial crack length, c , as a function of indentation load, P . Key: \square a , \circ c from reference 14, \blacksquare a , \bullet c from the present work.

close to the threshold region the strength distribution becomes bimodal, *i.e.* in high strength specimens failure is initiation controlled; in low strength specimens failure results from crack "pop-in" followed by subcritical crack growth (propagation controlled failure).⁵ We observed that the results for subthreshold flaws measured in two point and four point bending do not form one continuous line. The results from the four point apparatus are calculated assuming small deflections of the fiber. However, near the threshold region the fibers are strong enough to withstand large deflections so that the simple analysis is not adequate. Further development of the four point technique is in progress. It should be noted that the threshold in Dabbs and Lawn's study represented a transition in the specimen type and test technique as well in the indentation flaw behavior. It is still not clear how much of the discontinuity at the threshold can be attributed to the change in strength behavior and how much is due to changes in measurement technique and specimen geometry. Certainly, while our results do exhibit a sub-/postthreshold discontinuity in behavior at 0.5 and 1 N loads (*i.e.* a bimodal strength distribution), they also show a discontinuity in subthreshold behavior when the test technique is changed.

By considering the influence of the residual stresses on postthreshold radial cracks, Cook and Lawn¹⁵ determined that the relationship between inert strength (strain to failure) and indentation load is given by

$$\epsilon_f P^{1/3} = \lambda \quad (3)$$

where λ is a material constant depending on the Young's modulus, E , hardness, H and toughness, K_{IC} . Jakus *et al.*⁹ proposed a model for the strength of subthreshold flaws and obtained a reasonable fit to their data. Interestingly, the solid line in Fig. 9 through the subthreshold data has a slope of $-1/3$ so that a relationship of the form given by Eq. 3 appears to fit for subthreshold flaws as well (though these data were not for inert strength). A line of slope $-1/3$ also fits Jakus' inert strength data reasonably well though the data do not span a sufficiently wide range of load to confirm the fit.

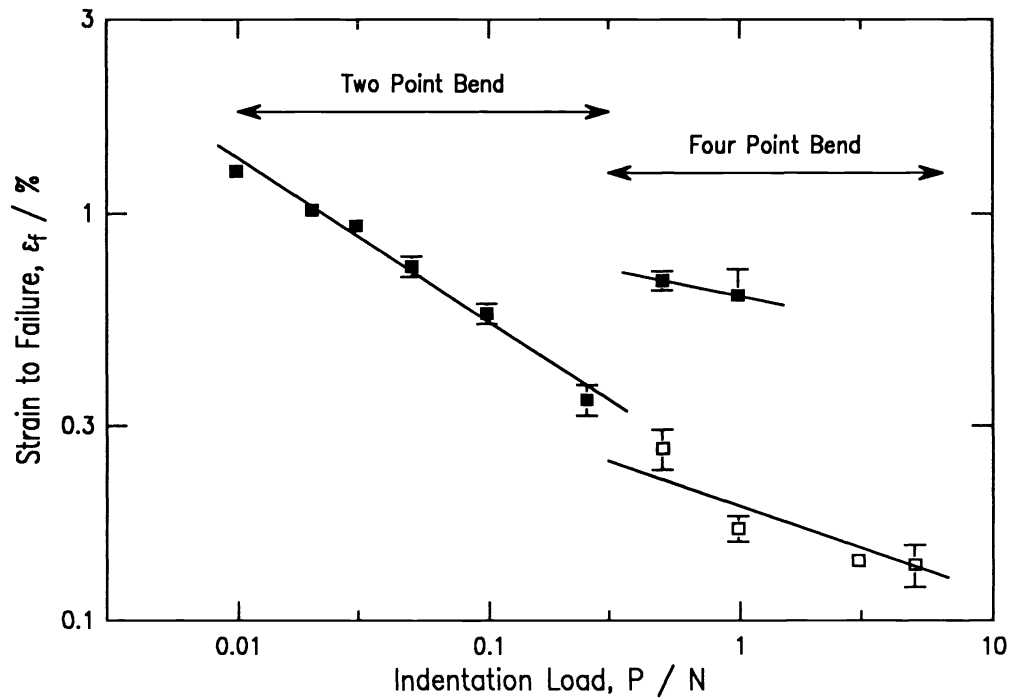


Fig. 9. Strain to failure versus indentation load at a strain rate of 0.036 %/min. Key: ■ subthreshold, □ postthreshold flaws.

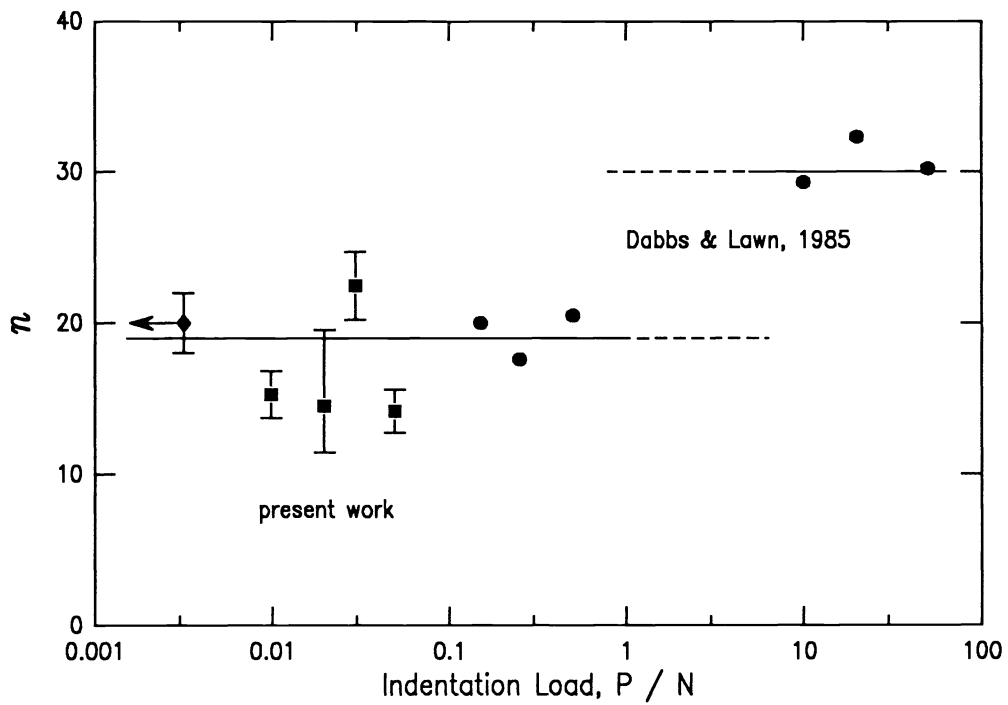


Fig. 10. Dynamic stress corrosion parameter, n , as a function of indentation load, P . Key: ■ present work, ● reference 5, ◆ pristine fiber.

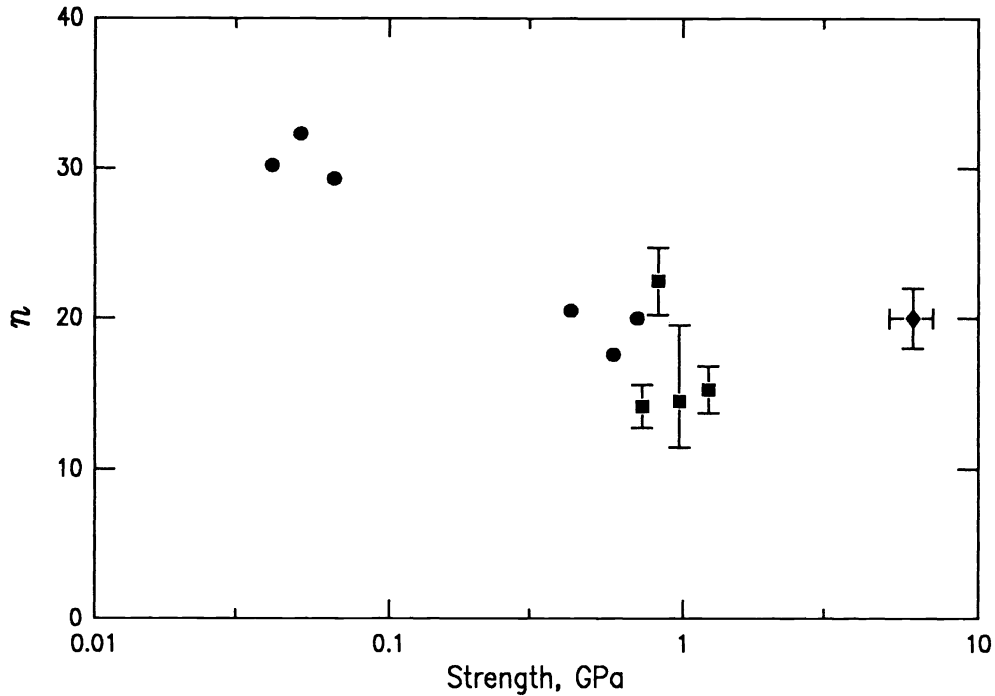


Fig. 11. Dynamic stress corrosion parameter, n , as a function of fiber strength. Key: ■ present work, ● reference 5, ◆ pristine fiber.

Fig. 10 shows the dynamic fatigue parameter, n , as a function of indentation load, P , for both published data and the present work. Also shown is the value of 20 widely accepted for pristine fiber with an effective zero indentation load. Within experimental uncertainty, n is approximately 20 throughout the subthreshold region. Fig. 11 shows the data for n of Fig. 10 reinterpreted in terms of the fiber strength. From the plots, we can see that the stress corrosion parameter n is not varying with indentation load and fiber strength. The gap between 1 N and 10 N of data can be filled by testing the dynamic fatigue behavior of indented fiber through the four point bending technique.

4. CONCLUSIONS

The indentation technique is an exciting approach to simulate the fatigue behavior of long length weak fiber by introducing flaws of controlled size. Our work has extended the indentation load down to ~ 10 mN in the subthreshold region where we find a stress corrosion parameter, n , around 20. We now have the opportunity to examine the fatigue behavior of fiber at strength typical of proof test levels. Continuing work will examine subthreshold flaws at very low indentation load to determine their relationship - if any - to pristine fiber behavior.

5. ACKNOWLEDGEMENTS

This work was supported in part by the Fiber Optic Materials Research Program at Rutgers University and in part by the New Jersey State Commission on Science and Technology. The authors are grateful to T. Rich of Fiberguide Industries, Stirling, NJ, for providing the fiber specimens used in this study.

6. REFERENCES

- 1 C. R. Kurkjian, J. T. Krause and U. C. Paek, "Tensile strength characteristics of "Perfect" silica fibers", *J. de Phys.* **43** [12] C9-585-586 (1982).
- 2 M. J. Matthewson, V. V. Rondinella, B. Lin and S. W. Keyes, "Cation effects on the strength of fused silica optical fiber" *J. Am. Ceram. Soc.*, in press.
- 3 C. R. Kurkjian, J. T. Krause and M. J. Matthewson, "Strength and fatigue of silica optical fibers," *J. Lightwave Tech.* **7** [9] 1360-1370 (1989).
- 4 H. H. Yuce, A. J. Colucci, P. L. Key and M. A. Andrejco, "Strength and fatigue behavior of low strength optical fibers" *Proc. OFC 89*, paper WA2 (1989).
- 5 T. P. Dabbs, B. R. Lawn, "Strength and fatigue properties of optical glass fibers containing microindentation flaws," *J. Am. Ceram. Soc.* **68** [11] 563-569 (1985).
- 6 R. F. Cook and G. M. Pharr, "Direct observation and analysis of indentation cracking in glasses and ceramics," *J. Am. Ceram. Soc.* **73** [4] 787-817 (1990).
- 7 M. J. Matthewson and C. R. Kurkjian, "Environmental effects on the static fatigue of silica optical fiber," *J. Am. Ceram. Soc.* **71** [3] 177-183 (1988).
- 8 B. R. Lawn and A. G. Evans, "A model for crack initiation in elastic/plastic indentation fields," *J. Mat. Sci.* **12** [11] 2195-2199 (1977).
- 9 K. Jakus, J. E. Ritter, Jr., S. R. Choi, T. Larder and B. R. Lawn, "Failure of fused silica fibers with subthreshold flaws," *J. Non-Cryst. Solids* **102** 82-87 (1988).
- 10 M. J. Matthewson, C. R. Kurkjian and S. T. Gulati, "Strength measurement of optical fibers by bending," *J. Am. Ceram. Soc.* **69** [11] 815-821 (1986).
- 11 H. H. Yuce, M. E. Melczer and P. L. Key, "Mechanical properties of optical fibers in bending" *Proc. 7th Int. Conf. Integrated Optics, Proc. SPIE 2 44* (1989).
- 12 P. W. France, M. J. Paradine, M. H. Reeve and G. R. Newns, "Liquid nitrogen strengths of coated optical fibers," *J. Mat. Sci.* **15** 825-830 (1980).
- 13 B. Fortunati and M. J. Matthewson, "Temperature dependence of optical fiber strength" *Am. Ceram. Soc. Bull.* **69** (3) 511, paper 2-JXII-90 (1990).
- 14 T. P. Dabbs and D. B. Marshall, B. R. Lawn, "Flaw generation by indentation in glass fibers," *J. Am. Ceram. Soc.* **63** [3-4] C224-225 (1980).
- 15 R. F. Cook and B. R. Lawn, "Controlled indentation flaws for construction of toughness and fatigue master maps," in "Methods for assessing the structural reliability of brittle materials," ASTM-STP 844, ed. by S. W. Freiman, C. M. Hudson, ASTM, pp22-42 (1984).